Since January 2020 Elsevier has created a COVID-19 resource centre with free information in English and Mandarin on the novel coronavirus COVID-19. The COVID-19 resource centre is hosted on Elsevier Connect, the company's public news and information website.

Elsevier hereby grants permission to make all its COVID-19-related research that is available on the COVID-19 resource centre - including this research content - immediately available in PubMed Central and other publicly funded repositories, such as the WHO COVID database with rights for unrestricted research re-use and analyses in any form or by any means with acknowledgement of the original source. These permissions are granted for free by Elsevier for as long as the COVID-19 resource centre remains active.

Biochemistry and Biophysics Reports 29 (2022) 101187

Contents lists available at ScienceDirect

Biochemistry and Biophysics Reports

journal homepage: www.elsevier.com/locate/bbrep

Iota-carrageenan extracted from red algae is a potent inhibitor of SARS-CoV-2 infection in reconstituted human airway epithelia

David Bovard [b,1], Marco van der Toorn [b,1], Walter K. Schlage [a], Samuel Constant [c], Kasper Renggli [b], Manuel C. Peitsch [b], Julia Hoeng [b,*]

[a] Biology Consultant, Max-Baermann-Str. 21, 51429, Bergisch Gladbach, Germany
[b] PMI R&D, Philip Morris Products S.A, Quai Jeanrenaud 5, 2000, Neuchâtel, Switzerland
[c] Epithelix Sarl, 18 Chemin des Aulx, Plan-les-Ouates, 1228, Geneva, Switzerland

ARTICLE INFO

Keywords:
SARS-CoV-2
Iota-carrageenan
Nasal epithelium
Bronchial epithelium
Air–liquid interface
COVID-19
Nasal spray

ABSTRACT

Iota-carrageenan (IC) nasal spray, a medical device approved for treating respiratory viral infections, has previously been shown to inhibit the ability of a variety of respiratory viruses, including severe acute respiratory syndrome coronavirus 2 (SARS-CoV-2), to enter and replicate in the cell by interfering with the virus binding to the cell surface. The aim of this study was to further investigate the efficacy and safety of IC in SARS-CoV-2 infection in advanced *in vitro* models of the human respiratory epithelium, the primary target and entry port for SARS-CoV-2. We extended the *in vitro* safety assessment of nebulized IC in a 3-dimensional model of reconstituted human bronchial epithelium, and we demonstrated the efficacy of IC in protecting reconstituted nasal epithelium against viral infection and replication of a patient-derived SARS-CoV-2 strain. The results obtained from these two advanced models of human respiratory tract epithelia confirm previous findings from *in vitro* SARS-CoV-2 infection assays and demonstrate that topically applied IC can effectively prevent SARS-CoV-2 infection and replication. Moreover, the absence of toxicity and functional and structural impairment of the mucociliary epithelium demonstrates that the nebulized IC is well tolerated.

1. Introduction

Coronavirus disease 2019 (COVID19), caused by the severe acute respiratory syndrome coronavirus 2 (SARS-CoV-2), is an ongoing pandemic, with more than 212 million confirmed cases and more than 4.4 million deaths worldwide as of week 33, 2021 [1]. While most patients develop mild symptoms, some develop severe symptoms like pneumonia, respiratory failure, shock, and multiorgan dysfunction. The high mortality of patients admitted to critical care with severe acute SARS-CoV-2 infection has been attributed to a combination of hyper-inflammatory syndromes, coagulation disorders, and pathological activation of immunological pathways leading to cytokine release syndrome [2,3].

There is an urgent need for effective, early treatments that have both antiviral and disease-modifying actions to limit the pressure that severe COVID-19 cases place on healthcare infrastructure [4–7]. While vaccination is the most efficacious route for primary prevention of COVID-19, intranasal or intraoral delivery of antiviral agents may be an important additional approach for preventing infection and the spread of SARS-CoV-2 and other respiratory viruses at their sites of entry, i.e., the nose and throat [7,8]. Indeed it has been demonstrated that the human angiotensin I-converting enzyme 2 (hACE2) receptor, recognized by the spike protein of SARS-CoV-2 for initiating infection, is highly expressed in the nasal and oral mucosa [9], and, accordingly, SARS-CoV-2 titers are extremely high in the nose and throat of infected patients [10]. Along the lines of this strategy, a number of agents with quite different mechanisms of action have recently been or are still being tested for repurposing in clinical trials, [7,8,11].

Abbreviations: IC, Iota-carrageenan; SARS-CoV-2, severe acute respiratory syndrome coronavirus 2; COVID19, Coronavirus disease 2019; hACE2, human angiotensin I-converting enzyme 2; 3D, 3-dimensional; NHBE, normal human bronchial epithelial; ALI, air–liquid interface; PBS, phosphate-buffered saline; TEER, transepithelial electrical resistance; CBF, ciliary beating frequency; LDH, lactate dehydrogenase; DMMB, Dimethylmethylene blue; MOI, multiplicity of infection; BE, before exposure; AE, after exposure; SSPL, spike-pseudotyped lentivirus.

* Corresponding author.
E-mail address: Julia.hoeng@pmi.com (J. Hoeng).

[1] These authors contributed equally to the manuscript.

https://doi.org/10.1016/j.bbrep.2021.101187
Received 15 November 2021; Received in revised form 9 December 2021; Accepted 9 December 2021
Available online 15 December 2021
2405-5808/© 2021 The Authors. Published by Elsevier B.V. This is an open access article under the CC BY-NC-ND license (http://creativecommons.org/licenses/by-nc-nd/4.0/).

Iota-carrageenan (IC), a natural linear sulfated polysaccharide extracted from edible red seaweed, can be used as a potential agent for prevention and management of a broad range of respiratory viral infections, including SARS and COVID-19 [8,12–16]. The mechanism of action of IC is nonspecific because its highly charged macromolecules bind to the viral surface and thereby prevent functional adhesion of the viral binding proteins with their cellular receptors, which is a prerequisite for cellular entry (internalization) and replication of the virus [14,16]. Moreover, IC has not been observed to possess pharmacological, immunological, or toxicological activity, and, because it is not absorbed or metabolized by cells, IC can be considered a safe topical antiviral treatment [14].

IC has demonstrated excellent translatability of its *in vitro* inhibition of viral infection into clinical efficacy [17–20]. IC has been approved as a medical device and may be administered as a nasal spray, mouthwash, or lozenge to treat viral infections of the respiratory tract [14,21]. Local administration of antiviral agents to the respiratory tract is desirable, as it helps maintain a high local concentration at the primary site of infection—e.g., airway respiratory epithelium—while keeping the systemic load low, unlike drugs that require systemic administration (e.g., remdesivir) [22]. Locally administered antiviral products may provide a two-fold benefit. First, they may prevent viral infection via the nasal route in healthy individuals by shielding the cellular surfaces [14]. Second, upon onset of symptoms, the product may prevent the viral particles released by infected cells from colonizing new cells (such as olfactory and respiratory epithelial cells) that could allow the pathogen to spread to new pathways and end up reaching the cardiovascular system or to infect more cells of the respiratory epithelium on its way to the lower respiratory system [14].

In this study, we have employed advanced 3-dimensional (3D) models of human nasal and bronchial epithelium to demonstrate the strong antiviral activity of IC and the absence of detectable adverse effects on the functional and structural integrity of the tissue.

2. Materials & methods

2.1. Human 3D airway cultures

Primary normal human bronchial epithelial (NHBE) cells (Lonza, Basel, Switzerland) from a 60-year-old male black donor were isolated and cultured on 6.5-mm-diameter collagen I-coated Transwell® inserts (Corning, Corning, NY, USA) as previously described [23,24]. The cultures were considered mature after 4 weeks at the air–liquid interface (ALI) and used for experiments between weeks 4 and 20 after air-lift.

For the nasal cultures used in the viral infection study, mature MucilAir™-Pool (Epithelix Sarl, Geneva, Switzerland) cultures, obtained from a pool of 14 different donors who underwent polypectomy, were expanded by two passages and cultured at the ALI in chemically defined, serum-free MucilAir™ culture medium (Epithelix Sarl) in 24-well plates with 6.5-mm Transwell® inserts (Corning) as previously described [25].

2.2. Exposure to nebulized or liquid IC

IC (GMP quality) was a generous gift from Dr. Eva Prieschl-Grassauer (Marinomed Biotech AG, Korneuburg, Austria). For testing the epithelial integrity of the bronchial epithelial cultures, a solution of 0.04, 0.08, 0.15, or 0.3 mg/mL IC in phosphate-buffered saline (PBS) was nebulized using the VITROCELL Cloud 12 system (VITROCELL Systems GmbH, Waldkirch, Germany), which led to an average deposition of 0.5–5 μg IC per 0.33 cm^2. This was followed by a 48-h incubation (Fig. 1). Nasal epithelial cells infected with SARS-CoV-2 were apically exposed to an IC solution (0.12 or 0.36 mg/mL) or vehicle (OptiMEM) by pipetting 20 μL of the solution/vehicle onto each culture insert as indicated under "Virus infection studies".

2.3. Dimethylmethylene blue (DMMB) assay

We used the DMMB assay to measure the concentration of IC deposited in the exposed bronchial cultures. For the assay, a 1-L solution containing 16 mg DMMB, 3.04 g glycine, 1.6 g NaCl, and 0.1 M acetic acid (all from Merck, Buchs, Switzerland) was prepared. Stainless steel inserts were filled with 200 μL of PBS and exposed to IC during the cell culture exposure runs. At the end of exposure, 20 μL of PBS from each of these inserts was transferred to a multiwell plate with a clear bottom, and 200 μL of the DMMB solution was added to each well of the plate. The absorbance was measured at 525 nm immediately after DMMB addition. The IC concentration was extrapolated from a standard curve.

2.4. Ciliary beating frequency (CBF) of bronchial epithelial cultures

Before and after IC exposure, CBF and the active area of ciliary beating were measured (Fig. 1) using an inverted microscope (Zeiss, Oberkochen, Germany) with a 4X objective and a 37 °C chamber; the microscope was connected to a high-speed camera (Basler AG, Ahrensburg, Germany). Short movies (512 frames at 120 images per second) were analyzed using the SAVA analysis software (Ammons Engineering, Clio, MI, USA).

2.5. Transepithelial electrical resistance (TEER)

TEER was measured before and after IC exposure. Culture medium (200 μL) was added to the apical compartment of the nasal and bronchial cultures, and resistance was measured with an EVOM voltohmmeter (World Precision Instruments, Sarasota, FL, USA) in combination with chopstick electrodes. Resistance values (Ω) were converted to TEER ($\Omega.cm^2$) by using the following formula: TEER ($\Omega.cm^2$) = (resistance value (Ω) – 100 (Ω)) x 0.33 (cm^2), where 100 Ω is the resistance of the

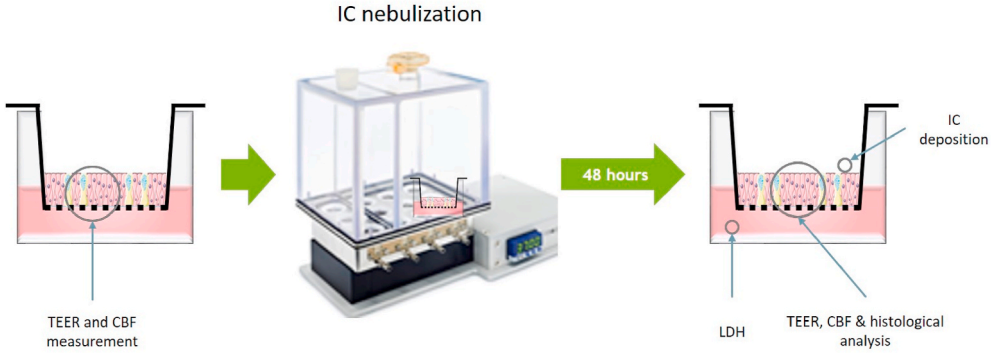

Fig. 1. Experimental design for assessing the safety of nebulized IC in bronchial cultures. TEER, transepithelial electrical resistance; CBF, ciliary beating frequency; IC, iota-carrageenan; LDH, lactate dehydrogenase.

membrane obtained with a cell-free insert and 0.33 cm^2 the total surface area of the membrane.

2.6. Lactate dehydrogenase (LDH) measurement in bronchial epithelial cultures

LDH was measured (LDH-Glo™ Cytotoxicity Assay, Promega, Madison, WI, USA) in the basolateral medium of cultures 48 h after exposure to nebulized IC. The values were normalized against the activity in bronchial tissues exposed to PBS (0%) and 2% Triton X-100 (Merck) for 24 h (100%).

2.7. Histological processing of bronchial epithelial cultures

The histological analysis procedure has been described previously [26]. Briefly, 5-μm perpendicular sections of formalin-fixed tissues were stained with hematoxylin-eosin/Alcian blue, and digitally imaged using the NanoZoomer 2.0 slide scanner (Hamamatsu Photonics, Hamamatsu, Japan).

2.8. Virus infection studies

All experiments involving the infectious SARS-CoV-2 were conducted by VirNext (Lyon, France) in their biosafety level 3 facilities, in accordance with the Declaration of Helsinki and with approval from the local ethics commission. The SARS-CoV-2 strain used in this study was isolated by directly inoculating monolayer VeroE6 cells with a nasal swab sample collected from Bichat Claude Bernard Hospital in Paris, France. The complete viral genome sequence was determined using the Illumina MiSeq sequencing technology and deposited in the GISAID EpiCov database (https://www.gisaid.org/) under the reference Beta-CoV/France/IDF0571/2020 [27].

To assess the potential protective effect of IC against SARS-CoV-2 infection, nasal MucilAir™-Pool cultures were exposed to different doses of IC at their apical surface by pipetting as follows: pre-incubation with IC for 1h, followed by virus inoculation (150 μL of solution at a theoretical multiplicity of infection (MOI) of 0.1, i.e., 50,000 TCID50 for an average of 500,000 cells) for 1h, then washing the apical side to remove non-attached viruses, after washing apical IC was applied again, and repeated at 24h. Virus-containing apical wash (10 min, 200 μL) was collected at 48h for analysis, thereafter IC treatment was repeated until 72h after inoculation. A final apical wash was collected for virus analysis, and TEER was measured at 72h.

As a reference, the broad-spectrum antiviral medication remdesivir (5 μM) was added to the basolateral medium (to mimic its systemic administration post-infection) of some nasal cultures 1 h after inoculation with SARS-CoV-2. OptiMEM-DMSO was used for the positive (inoculation with virus) and negative (no inoculation with virus) control.

2.9. Real-time Taqman probe RT-PCR for virus quantification

From the 200 μL apical washes, 140 μL was used for viral RNA extraction with the QIAamp® Viral RNA kit (Qiagen, Hilden, Germany); the RNA was eluted into 60 μL of buffer. Then, the viral RNA (2 μL) was quantified by qRT-PCR (EXPRESS One-Step Superscript™ qRT-PCR Kit, Thermo Fisher Scientific) by using the mastermix in the kit and two ORF1b-nsp14-specific primers (5′-TGGGGYTTTACRGGTAACCT-3′; 5′-AACRCGCTTAACAAAGCACTC-3′) and a SARS-CoV-2 probe (5′-FAM-TAGTTGTGATGCWATCATGACTAG-TAMRA-3′) designed by the School of Public Health/University of Hong Kong (Leo Poon, Daniel Chu and Malik Peiris). The reaction was run on the StepOnePlus™ Real-Time PCR system (Applied Biosystems, Waltham, MA, USA). Ct data were determined, and relative changes in gene expression were calculated by the 2-ΔCt method and reported as fold reduction relative to the mean of the values of vehicle-treated infected inserts.

3. Results

3.1. Nebulized IC does not affect tissue function or integrity and is nontoxic

We first used the colorimetric DMMB assay to determine the amount of deposited IC in PBS-filled inserts. The results indicated that up to 5 μg IC (or 15 μg IC/cm^2; approximately 10% of the initially nebulized dose) was deposited in the apical compartment of the culture inserts (Fig. 2A). Analysis of medium from the basal compartment demonstrated that IC was not transferred across the filter membrane, which was impermeable to the IC macromolecules (data not shown). The safety of the nebulized solution was investigated using endpoints indicative of epithelial function (CBF), integrity (TEER and histological structure), and viability (LDH release). Bronchial tissues exposed to nebulized IC, independent of the IC dose, presented significantly higher CBF after exposure to IC than before exposure (Fig. 2B). For the active area of ciliary beating in the same tissues, the post-IC exposure values were all in the same range (80% or above), although the pre-exposure values had varied among the inserts (Fig. 2C). The TEER values showed no change after exposure to IC, independent of the dose; all TEER values were in the normal range (above 300 Ωcm^2; Fig. 2D). The lack of cytotoxicity was confirmed by absence of LDH in the medium of all IC dose groups (Fig. 2E).

Histology revealed no adverse morphological changes at 48 h after exposure to nebulized IC relative to PBS-exposed bronchial tissues. All tissues showed similar ciliation and a comparable proportion of goblet cells (within the usual range of variability) and no evidence of hyperplasia. Other markers of cytotoxicity such as vacuole formation in the epithelium, loss of cell polarization or detachment of the tissue from the insert membrane were not visible even at the maximum dose tested (Fig. 3).

3.2. IC protects nasal epithelial cells against SARS-CoV-2 infection

TEER measurement indicated no change in epithelial integrity between SARS-CoV-2-infected and non-infected cells at any time point (Fig. 4A). The cultures showed apparently higher TEER values 48 and 72 h after exposure to remdesivir and IC, respectively; but this was due to a decrease in TEER in the vehicle controls rather than changes in the treated cultures, which, in fact, retained their baseline TEER values.

RT-PCR analysis of the apical washes of the MucilAir™ inserts demonstrated significantly lower apical SARS-CoV-2 genome copy numbers with both concentrations of IC at both time points in comparison to the controls (Fig. 4B). The magnitudes of reduction (vs. vehicle control) were 4.4 and 5.5 log10 with the high IC concentration and 3.5 and 4.9 log10 with the low IC concentration at 48 and 72 h post-treatment, respectively. Remdesivir, used as the reference, reduced apical SARS-CoV-2 genome copy numbers at both time points by 2 log10 at 48 h and 3.8 log10 at 72 h post-infection (vs. the vehicle control).

4. Discussion

The aim of this study was to further investigate the efficacy and safety of IC treatment on SARS-CoV-2 infection by using advanced *in vitro* models of human respiratory epithelium, the primary target and entry port of SARS-CoV-2.

The experimental models were 3D cultures of reconstituted bronchial and nasal epithelia, representing the surface of the human upper respiratory tract. These air-lifted *in vitro* cultures exhibit the organotypic differentiation of respiratory epithelium—including a pseudostratified structure composed of ciliated cells, mucus-producing goblet cells, and basal (reserve) cells [28]—as well as important functional traits such as ciliary beating and barrier activities against inhaled molecules and particles [29].

In our safety assessment, we exposed human bronchial epithelial cultures [23,24] to defined doses of nebulized IC which were

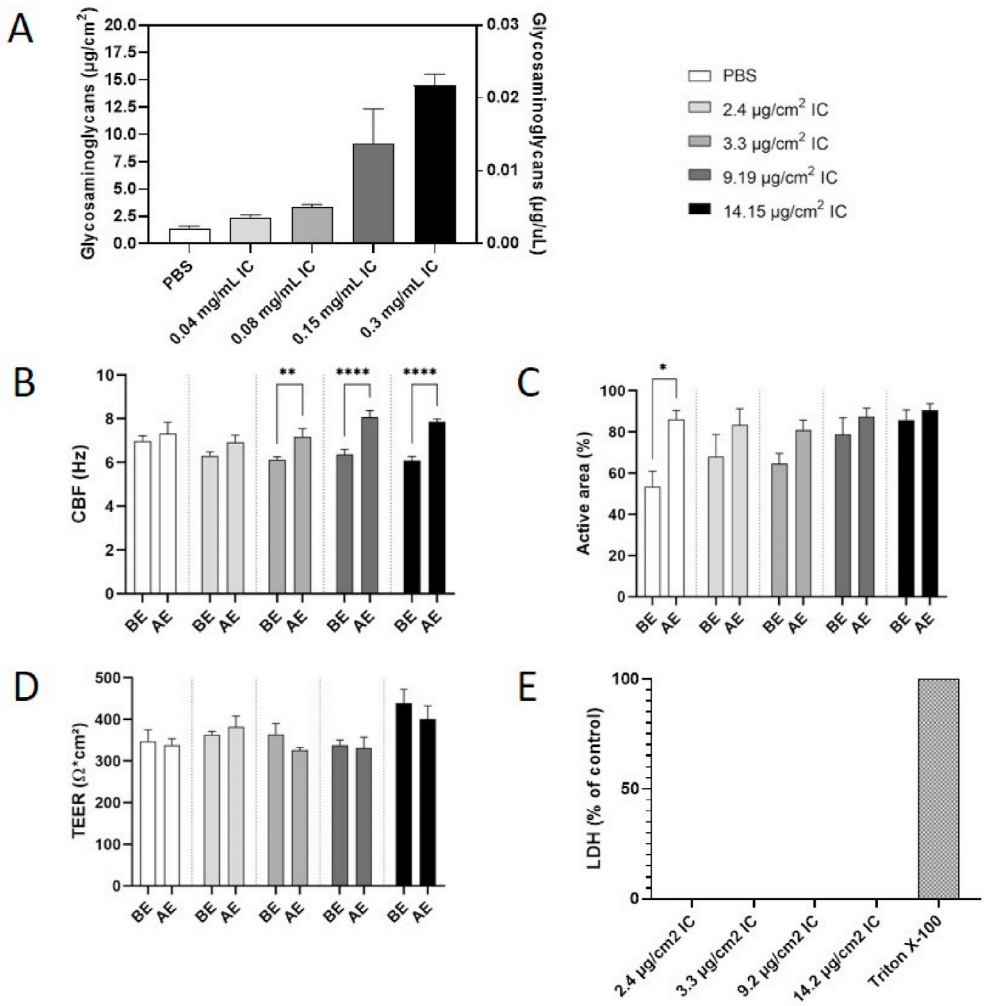

Fig. 2. A) Mass (left y-axis) and concentration (right y-axis) of IC deposited in the apical compartment of bronchial epithelial cultures exposed to aerosolized IC. B) CBF and C) active area of ciliary beating before and 48 h after exposure to nebulized IC. Each condition was statistically compared with vehicle treatment by two-way analysis of variance with Dunnett's multiple comparison post-tests (Prism 9.0 GraphPad; *$p < 0.05$, **$p < 0.01$, ****$p < 0.001$). D) TEER before and 48 h after exposure to nebulized IC. E) LDH in medium of bronchial cultures 48 h after exposure to nebulized IC; 0% corresponds to the value measured in tissues exposed to PBS and 100% to the value measured in tissues incubated for 24 h with 2% Triton X-100. Data are presented as mean ± standard error of the mean for n = 3 independent inserts. BE, before exposure; AE, 48 h after exposure; IC, iota-carrageenan; PBS, phosphate-buffered saline; TEER, transepithelial electrical resistance; CBF, ciliary beating frequency; LDH, lactate dehydrogenase.

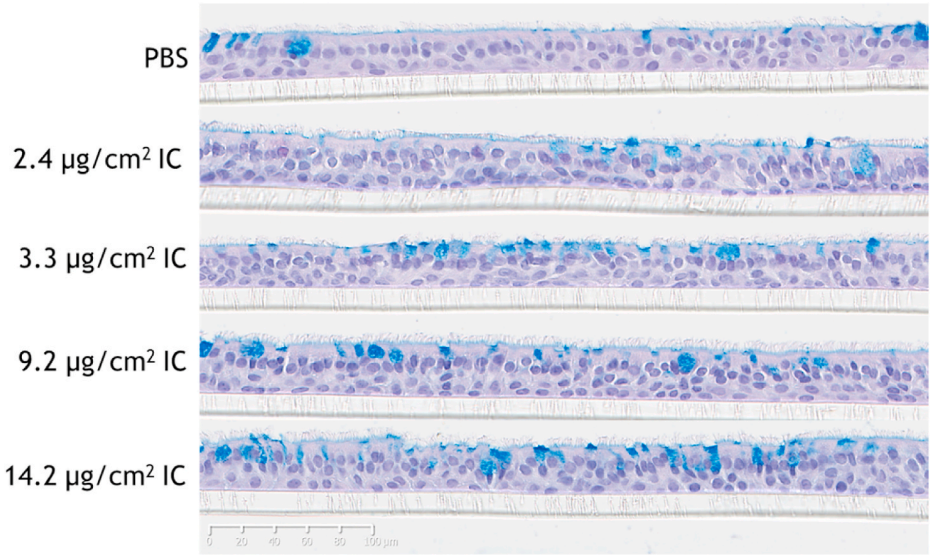

Fig. 3. Histological findings in bronchial epithelial cultures. The bronchial cultures were washed 3 times with PBS before being histologically processed and stained with hematoxylin, eosin, and Alcian blue 48 h after exposure to nebulized IC. Scale bar, 100 µm. IC, iota-carrageenan. (For interpretation of the references to color in this figure legend, the reader is referred to the Web version of this article.)

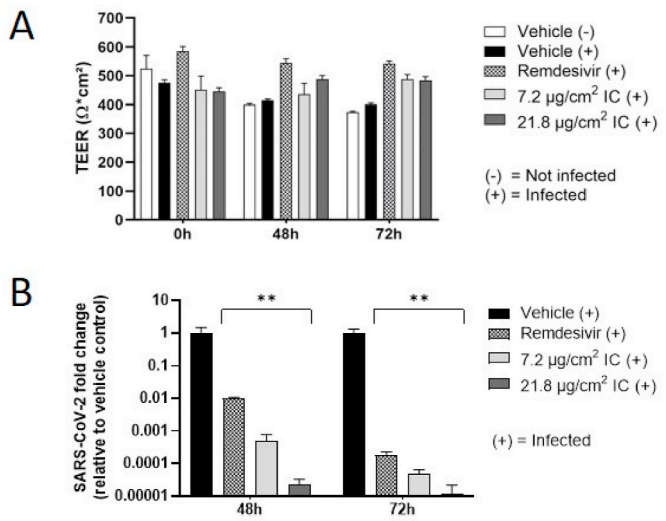

Fig. 4. Antiviral activity of IC against SARS-CoV-2 infection in nasal epithelial (MucilAir™-Pool) cultures. A) Effect of IC on TEER before and 48 and 72 h after SARS-CoV-2 infection. B) Relative SARS-CoV-2 genome copy numbers on the apical side of cultures with 1-h pretreatment and repeated apical exposure to IC. As a reference, remdesivir (5 μM) was added to the basolateral medium. Data are presented as mean ± standard error of the mean for n = 12 independent inserts. Each condition was statistically compared with vehicle treatment by two-way analysis of variance with Dunnett's multiple comparison post-tests (Prism 9.0 GraphPad; $^{**}p < 0.01$). IC, iota-carrageenan; TEER, transepithelial electrical resistance.

reproducibly generated and administered using the VITROCELL Cloud device [30]. Our results indicated the absence of (i) toxicity (LDH release), (ii) structural changes (histology), and (iii) functional changes in both ciliary surface clearance (CBF and active area of ciliary beating) and tightness of the epithelial barrier (TEER). That IC lacks cytotoxicity (endpoint: cell viability) has recently been demonstrated in monolayer cultures of Vero B4 cells treated with IC concentrations up to 100 μg/mL in the culture medium [14]; these concentrations are considerably higher than the maximum IC concentration (30 μg/mL in the apical compartment) used in the present study. As IC does not enter the systemic circulation, the apical exposure of reconstructed epithelia more closely mimics real-life exposure conditions than submerged monolayer cells. The 3D epithelial model is also capable of mucociliary clearance, which was not impaired after IC treatment, in fact there was a slight increase in CBF and cilia beating active area. Since the mucociliary clearance was also increased in cultures exposed to nebulized PBS, the effect was likely caused by aqueous dilution resulting in a change in mucous viscosity.

Concerning the epithelial barrier function, TEER is a dynamic parameter, typically ranging between 200 and 600 Ωcm^2 in respiratory epithelia [31]. An increase in TEER reflects a blockage of ion channel activities, and a notable decrease (<100 Ωcm^2) occurs when cellular junctions are disrupted or when holes are created in the epithelia, which is usually associated with an increase in LDH release or lower cell viability. In this study, the epithelia showed neither any disturbance in TEER nor any effect on their impermeability to large molecules (IC) or permeability for small molecules (fluorescein, data not shown); these data are in full agreement with previous findings from studies using explanted bovine nasal mucosa [32].

The viral infection studies were conducted in reconstructed nasal epithelial cultures blended from 14 donors (MucilAir™-Pool). Like the 3D bronchial cultures, MucilAir™ is composed of basal cells, ciliated cells, and mucus cells at the same proportions as those observed *in vivo* [25]. They are functionally differentiated, secrete mucus, and are electrically tight (TEER >200 Ωcm^2), with the main epithelial ionic channels preserved [25].

A previous IC antiviral study used monolayer cultures of ACE2-HEK cells infected with a SARS-CoV-2 spike-pseudotyped lentivirus (SSPL) and Vero B4 cells infected with patient-derived SARS-CoV-2 as the test models [14], while another study used ALI cultures of human airway epithelial cells infected with patient-derived SARS-CoV-2 [33], as we did in our study. We confirmed the antiviral activity of IC against a patient-derived active SARS-CoV-2 strain by leveraging a differentiated nasal epithelial model. The epithelia were treated by pipetting an IC solution onto the apical side at effective doses (7.2 and 21.8 μg/cm^2) comparable to those we used in the safety assessment of aerosolized IC in bronchial epithelial cultures. To assess the antiviral efficacy of IC against SARS-CoV-2 infection, we measured the apical viral replication (genome copy number) and tissue integrity in infected IC-treated nasal cultures. Neither viral infection nor IC impaired tissue integrity/barrier function in this study, whereas SARS-CoV-2 has previously been reported to decrease TEER transiently and to induce ultrastructural changes in MucilAir nasal cultures [27]. IC treatment caused a strong reduction in virus replication (between 3.5 and 5.5 log10 relative to vehicle controls) in the SARS-CoV-2 genome copy number at both concentrations and both time points, thereby even exceeding the antiviral effect of the positive control, remdesivir. These findings confirm and complement previous *in vitro* data on IC efficacy in virus infection assays [14] by leveraging an advanced nasal respiratory epithelial model and a genuine SARS-CoV-2 strain and provide evidence that IC does not cause functional impairment or toxicity when applied topically to reconstituted bronchial epithelium as an inhalable aerosol.

In conclusion, our study demonstrates the potent antiviral effect of IC in MucilAir nasal cultures when it is applied before and repeatedly after infection with SARS-CoV-2. Moreover, the absence of toxicity or any functional or structural impairment of the bronchial mucociliary epithelium demonstrates that topical treatment with nebulized IC is well tolerated at the effective concentrations. Together with currently running clinical studies on the efficacy of an IC nasal spray in preventing SARS-Cov-2 infection or slowing down virus replication in the target tissues of the respiratory tract, these data may help evaluate IC's potential usefulness as a complementary treatment in cases where vaccination is not available or insufficient.

Funding

Philip Morris International is the sole source of funding and sponsor of this research.

Declaration of competing interest

The authors declare that they have no known competing financial interests or personal relationships that could have appeared to influence the work reported in this paper.

Acknowledgments

The authors would like to thank Manuel Rosa-Calatrava, Thomas Julien, and Blandine Padey at Vir Next for their excellent work with the infectious SARS-CoV-2, Eva Prieschl-Grassauer at Marinomed for providing the IC sample, and Martina Morokutti-Kurz (Marinomed) and Sindhoora Bhargavi Gopala Reddy for critical review of the manuscript.

References

[1] ECDC, COVID-19 situation update worldwide, as of week 23, updated 17 June 2021. 2021 [cited 2021 june 24, 2021]; Available from: https://www.ecdc.europa.eu/en/geographical-distribution-2019-ncov-cases.
[2] B. Hu, et al., Characteristics of SARS-CoV-2 and COVID-19, Nat. Rev. Microbiol. 19 (3) (2021) 141–154.
[3] S. Colafrancesco, et al., COVID-19 gone bad: a new character in the spectrum of the hyperferritinemic syndrome? Autoimmun. Rev. 19 (7) (2020) 102573.

[4] R.A. Giovane, et al., Current pharmacological modalities for management of novel coronavirus disease 2019 (COVID-19) and the rationale for their utilization: a review, Rev. Med. Virol. 30 (5) (2020) e2136.
[5] J.M. Sanders, et al., Pharmacologic treatments for coronavirus disease 2019 (COVID-19): a review, Jama 323 (18) (2020) 1824–1836.
[6] P.S. Kim, S.W. Read, A.S. Fauci, Therapy for early COVID-19: a critical need, Jama 324 (21) (2020) 2149–2150.
[7] M.J. Burton, et al., Antimicrobial mouthwashes (gargling) and nasal sprays administered to patients with suspected or confirmed COVID-19 infection to improve patient outcomes and to protect healthcare workers treating them, Cochrane Database Syst. Rev. 9 (9) (2020) Cd013627.
[8] C. Stathis, et al., Review of the use of nasal and oral antiseptics during a global pandemic, Future Microbiol. 16 (2) (2021) 119–130.
[9] I. Hamming, et al., Tissue distribution of ACE2 protein, the functional receptor for SARS coronavirus. A first step in understanding SARS pathogenesis, J. Pathol. 203 (2) (2004) 631–637.
[10] L. Zou, et al., SARS-CoV-2 viral load in upper respiratory specimens of infected patients, N. Engl. J. Med. 382 (12) (2020) 1177–1179.
[11] M.J. Burton, et al., Use of antimicrobial mouthwashes (gargling) and nasal sprays by healthcare workers to protect them when treating patients with suspected or confirmed COVID-19 infection, Cochrane Database Syst. Rev. 9 (2020) Cd013626.
[12] D. Bichiri, A.R. Rente, Â. Jesus, Safety and efficacy of iota-carrageenan nasal spray in treatment and prevention of the common cold, Med Pharm Rep 94 (1) (2021) 28–34.
[13] H. Hemilä, E. Chalker, Carrageenan Nasal Spray May Double the Rate of Recovery from Coronavirus and Influenza Virus Infections: Re-analysis of Randomized Trial Data, 2020.
[14] M. Morokutti-Kurz, et al., Iota-carrageenan neutralizes SARS-CoV-2 and inhibits viral replication in vitro, PLoS One 16 (2) (2021) e0237480.
[15] A. Leibbrandt, et al., Iota-carrageenan is a potent inhibitor of influenza A virus infection, PLoS One 5 (12) (2010) e14320.
[16] A. Grassauer, et al., Iota-Carrageenan is a potent inhibitor of rhinovirus infection, Virol. J. 5 (2008) 107.
[17] R. Eccles, et al., Efficacy and safety of an antiviral Iota-Carrageenan nasal spray: a randomized, double-blind, placebo-controlled exploratory study in volunteers with early symptoms of the common cold, Respir. Res. 11 (1) (2010) 108.
[18] T. Fazekas, et al., Lessons learned from a double-blind randomised placebo-controlled study with a iota-carrageenan nasal spray as medical device in children with acute symptoms of common cold, BMC Compl. Alternative Med. 12 (2012) 147.
[19] M. Ludwig, et al., Efficacy of a carrageenan nasal spray in patients with common cold: a randomized controlled trial, Respir. Res. 14 (1) (2013) 124.
[20] M. Koenighofer, et al., Carrageenan nasal spray in virus confirmed common cold: individual patient data analysis of two randomized controlled trials, Multidiscip Respir Med 9 (1) (2014) 57.
[21] M. Morokutti-Kurz, C. Graf, E. Prieschl-Grassauer, Amylmetacresol/2,4-dichlorobenzyl alcohol, hexylresorcinol, or carrageenan lozenges as active treatments for sore throat, Int. J. Gen. Med. 10 (2017) 53–60.
[22] O. Kavanagh, et al., Inhaled hydroxychloroquine to improve efficacy and reduce harm in the treatment of COVID-19, Med. Hypotheses 143 (2020) 110110.
[23] D. Bovard, et al., A lung/liver-on-a-chip platform for acute and chronic toxicity studies, Lab Chip 18 (24) (2018) 3814–3829.
[24] D. Bovard, et al., Comparison of the basic morphology and function of 3D lung epithelial cultures derived from several donors, Current Research in Toxicology 1 (2020) 56–69.
[25] S. Huang, L. Wiszniewski, S. Constant, The use of in vitro 3D cell models in drug development for respiratory diseases, in: I.M. Kapetanovic (Ed.), Drug Discovery and Development - Present and Future, InTech, Rijeka, Croatia, 2011, pp. 169–230.
[26] A.R. Iskandar, et al., 3-D nasal cultures: systems toxicological assessment of a candidate modified-risk tobacco product, ALTEX (2016).
[27] A. Pizzorno, et al., Characterization and treatment of SARS-CoV-2 in nasal and bronchial human airway epithelia, Cell Rep Med 1 (4) (2020) 100059.
[28] A. Baxter, et al., Targeted omics analyses, and metabolic enzyme activity assays demonstrate maintenance of key mucociliary characteristics in long term cultures of reconstituted human airway epithelia, Toxicol. Vitro 29 (5) (2015) 864–875.
[29] E. Iverson, et al., Leveraging 3D model systems to understand viral interactions with the respiratory mucosa, Viruses 12 (12) (2020).
[30] A.G. Lenz, et al., A dose-controlled system for air-liquid interface cell exposure and application to zinc oxide nanoparticles, Part. Fibre Toxicol. 6 (2009) 32.
[31] B. Srinivasan, et al., TEER measurement techniques for in vitro barrier model systems, J. Lab. Autom. 20 (2) (2015) 107–126.
[32] C. Graf, et al., Development of a nasal spray containing xylometazoline hydrochloride and iota-carrageenan for the symptomatic relief of nasal congestion caused by rhinitis and sinusitis, Int. J. Gen. Med. 11 (2018) 275–283.
[33] D. Schütz, et al., Carrageenan-containing over-the-counter nasal and oral sprays inhibit SARS-CoV-2 infection of airway epithelial cultures, Am. J. Physiol. Lung Cell Mol. Physiol. 320 (5) (2021) L750–l756.